Multiple Phosphorylated Variants of the High Molecular Mass Subunit of Neurofilaments in Axons of Retinal Cell Neurons: Characterization and Evidence for Their Differential Association with Stationary and Moving Neurofilaments

Susan E. Lewis and Ralph A. Nixon

Ralph Lowell Laboratories, Mailman Research Center, McLean Hospital, Belmont, Massachusetts 02178; and Department of Psychiatry and Program in Neuroscience, Harvard Medical School, Boston, Massachusetts 02115

Abstract. The 200-kD subunit of neurofilaments (NF-H) functions as a cross-bridge between neurofilaments and the neuronal cytoskeleton. In this study, four phosphorylated NF-H variants were identified as major constituents of axons from a single neuron type, the retinal ganglion cell, and were shown to have characteristics with different functional implications.

We resolved four major Coomassie Blue–stained proteins with apparent molecular masses of 197, 200, 205, and 210 kD on high resolution one-dimensional SDS–polyacrylamide gels of mouse optic axons (optic nerve and optic tract). Proteins with the same electrophoretic mobilities were radiolabeled within retinal ganglion cells in vivo after injecting mice intravitreally with [^{35}S]methionine or [^{3}H]proline. Extraction of the radiolabeled protein fraction with 1% Triton X-100 distinguished four insoluble polypeptides (P197, P200, P205, P210) with expected characteristics of NF-H from two soluble neuronal polypeptides (S197, S200) with few properties of neurofilament proteins. The four Triton-insoluble polypeptides displayed greater than 90% structural homology by two-dimensional α-chymotryptic iodopeptide map analysis and cross-reacted with four different monoclonal and polyclonal antibodies to NF-H by immunoblot analysis. Each of these four polypeptides advanced along axons primarily in the Group V (SCa) phase of axoplasmic transport. By contrast, the two Triton-soluble polypeptides displayed only a minor degree of α-chymotryptic peptide homology with the Triton-insoluble NF-H forms, did not cross-react with NF-H antibodies, and moved primarily in the Group IV (SCb) wave of axoplasmic transport. The four NF-H variants were generated by phosphorylation of a single polypeptide. Each of these polypeptides incorporated ^{32}P when retinal ganglion cells were radiolabeled in vivo with [^{32}P]orthophosphate and each cross-reacted with monoclonal antibodies specifically directed against phosphorylated epitopes on NF-H. When dephosphorylated in vitro with alkaline phosphatase, the four variants disappeared, giving rise to a single polypeptide with the same apparent molecular mass (160 kD) as newly synthesized, unmodified NF-H.

The NF-H variants distributed differently along optic axons. P197 predominated at proximal axonal levels; P200 displayed a relatively uniform distribution; and P205 and P210 became increasingly prominent at more distal axonal levels, paralleling the distribution of the stationary neurofilament network. Semiquantitative analyses of pulse-radiolabeled NF-H variants between 3 and 60 d after synthesis showed that P197 was the principal NF-H variant composing neurofilaments in the axonally transported wave as this wave advanced along axons at the optic nerve level. Long after the neurofilament transport wave had reached nerve terminals (60 d after injection), P210 and P205 remained prominently radiolabeled along axons, indicating that these variants were the major NF-H constituents of neurofilaments associated with the stationary cytoskeleton.

On the basis of these data, we propose that phosphorylation regulates the specific association of neurofilaments with different domains of the neuronal cytoskeleton. Changes in the phosphorylation state of NF-H during axoplasmic transport may represent one of the mechanisms that triggers the integration of moving neurofilaments into the stationary cytoskeleton.

Portions of this work have appeared in abstract form (1985. *Trans. Am. Soc. Neurochem.* 16:245a. [Abstr.]; 1987. *Soc. Neurosci. Abstr.* 13:1513a. [Abstr.]).

Address reprint requests to Dr. R. A. Nixon, Ralph Lowell Laboratories, Mailman Research Center, McLean Hospital, Belmont, MA 02178.

CYTOSKELETAL proteins in many tissues exhibit structural microheterogeneity. Isoforms of tubulin (6, 10, 46, 49, 68), actin (50), microtubule-associated proteins (23, 51, 68, 70), and other cytoskeletal proteins (13, 22, 39, 40, 54, 90), generated by genetic or posttranslational mechanisms, may display selectivity for a particular tissue or cell type or may appear at a specific stage of cellular development. In addition, multiple structural variants of a protein are sometimes observed within the same differentiated cell (23, 40, 80, 90). Although their presence within single cells could reflect the transition of a polypeptide from a precursor form to a fully functional state, variants arising by posttranscriptional or posttranslational processing may also amplify the range of functions that a single gene product serves in different sites within the cell.

Proteins made up of neurofilaments, the intermediate filaments of neurons, are extensively modified after synthesis (3, 30, 31, 59, 63, 64, 80, 81), and the complexity of these posttranslational processing events (1, 18, 60, 61, 66, 69, 84) holds important clues to the function of these cytoskeletal elements. Neurofilaments comprise three subunits (26, 78, 83, 85), referred to as high, middle, and low molecular mass neurofilament proteins (NF-H, NF-M, and NF-L, respectively),[1] to denote their relative molecular sizes (160–210, 140–160, and 70 kD). Microheterogeneity of the neurofilament triplet proteins is generated by limited proteolysis (58, 63), phosphorylation (4, 18, 20, 30, 41, 61, 66, 69), and dephosphorylation (60). The NF-H and NF-M subunits, in particular, are among the most highly phosphorylated proteins in the brain (8, 29, 30), and phosphorylated forms of NF-H and NF-M display different physicochemical properties from those of their unmodified counterparts (30, 32). Since most newly synthesized neurofilament proteins are destined for posttranslational modification and export into axons, it is unclear whether relatively unmodified neurofilament proteins are transient precursors to more mature polypeptides or represent functional constituents of the perikaryal cytoskeleton. Microdifferentiation of the neurofilament network has been suggested by the segregation in some neurons of relatively poorly phosphorylated neurofilaments within neuronal perikarya and extensively phosphorylated neurofilaments within axons (1, 2, 18, 19, 42, 60, 69, 80).

Evidence that NF-H and NF-M subunits continue to be modified (58, 60, 63, 66) as they advance along axons emphasizes that, even within the axon itself, the cytoskeleton is regionally specialized (6, 58). Functional as well as structural microdifferentiation of the axonal cytoskeleton is supported by observations that neurofilament subunits in central axons compose neurofilaments of two types (62). Neurofilaments in the process of translocation within the slowest phase of axoplasmic transport contribute to a lattice of neurofilaments that is part of the stationary cytoskeletal network along axons (59, 62). Stationary neurofilaments represent the predominant pool of neurofilaments in mature retinal ganglion cell neurons, and this network is particularly prominent in distal axonal regions (59, 62).

The existence of a stationary neurofilamentous cytoskeleton as well as moving neurofilaments implies that the interactions of these cytoskeletal elements during axoplasmic transport must be highly dynamic and tightly regulated. Posttranslational modifications of neurofilament proteins could coordinate these interactions by altering the affinity of neurofilaments for other cytoskeletal structures (28, 47, 53, 55, 74). Modifications of the high molecular mass neurofilament subunit may be particularly important for this process since NF-H subunits are believed to form cross-bridges that interconnect neurofilaments and possibly link these elements to other cytoskeletal components and membrane-bound organelles (25, 75, 88). Phosphate groups, for example, are added primarily to the hypervariable carboxy-terminal end of NF-H which protrudes from the neurofilament core and presumably interacts with other cytoskeletal proteins (8, 16, 32).

To further examine the cellular roles of NF-H and the significance of NF-H phosphorylation in regulating neurofilament organization and function, we used a combination of biochemical, cell biological, and immunological approaches to identify major forms of NF-H in retinal ganglion cells and to characterize certain properties of these variants. Earlier studies showed that NF-H migrates on two-dimensional gels as a diffuse, sometimes discontinuous spot suggesting the presence of multiple microheterogeneous forms (7, 12, 20). Recently, monoclonal antibodies were used to identify several differentially phosphorylated states of NF-H by immunoblot and immunocytochemical analysis (20, 42). In the present investigation, we used a range of criteria to identify different forms of NF-H in a single class of central neurons. In view of the complex dynamics of cytoskeletal elements during axoplasmic transport and maintenance of the axonal cytoskeleton, we focused on the microheterogeneity of NF-H specifically within axons. The results of this study establish the existence of multiple forms of NF-H, the probable mechanism for their generation, and possible functional correlates of this structural microheterogeneity.

Materials and Methods

Animals and Tissue Preparation

10–14-wk-old male or female mice of the C57BL/6J inbred strain were used in all experimental studies. Mouse breeding and maintenance and tissue dissections have been previously described (56, 63). The primary optic pathway, termed optic axons, consisted of (*a*) the optic nerve severed at the scleral surface of the eye, (*b*) the optic chiasm, and (*c*) part of the optic tract extending to, but not including, terminals in the lateral geniculate nucleus. The entire dissected segment was 10 mm long. In some studies, optic pathways were cut into consecutive 1.1-mm segments. Proteins soluble in 1% Triton X-100 solutions and Triton-insoluble cytoskeletal proteins were prepared from optic pathways by the method of Chiu and Norton (9) modified to include a 100,000 *g* final centrifugation instead of the usual 30,000 *g* centrifugation.

Tissue Preparation and One-dimensional SDS-PAGE

One-dimensional SDS-PAGE was performed by the procedure of Laemmli (36) using 320-mm slab gels containing 5–15 or 3–7% polyacrylamide gradients. Samples for electrophoresis were prepared under conditions designed to minimize proteolysis and protein loss. Samples were stored at −70°C in the presence of 50 μg/mg leupeptin, 0.5 mM PMSF, and 2.5 mg/ml aprotinin. To analyze unfractionated optic pathways in a single gel lane, a 2–3-mg wet weight of tissue (one optic pathway) was thawed in 150 μl of ice-cold Laemmli buffer (62.5 mM Tris HCl, pH 6.8, 10% glycerol, and 0.002% bromphenol blue) within a small glass homogenizer. After homogenization, the samples were incubated on ice for 10 min with 2 μg each of RNase and DNase. A volume of 10% SDS (40 μl) and 2-mercaptoethanol (7 μl) was then added and the samples were boiled for 10 min, cooled, and loaded on gels. In some cases proteins in polyacrylamide slices

1. *Abbreviations used in this paper*: NF-H, high molecular mass (200-kD) neurofilament protein; NF-M, middle molecular mass neurofilament protein; NF-L, low molecular mass neurofilament protein.

excised from SDS gels were subjected to a second electrophoresis. These slices were first equilibrated to pH 6.8 in several changes of a Tris-HCl buffer (62.5 mM, pH 6.8) containing 0.1% SDS. The slices were then homogenized and prepared as described above for tissue homogenates, but the RNase and DNase incubation step was omitted. Proteins on gels were stained with 0.1% Coomassie Brilliant Blue (Schwarz-Mann, Cambridge, MA) and destained as previously described (7).

Radiolabeling of Proteins in Retinal Ganglion Cells In Vivo

Mice were injected intravitreally with 15–25 μCi of [2,3-^{3}H]L proline (sp act, 30–50 Ci/mmol), 75 μCi of [^{35}S]methionine (sp act, 400 Ci/mmol), or 30 μCi of [^{32}P]orthophosphate (sp act, 1,000 Ci/mmol) (New England Nuclear, Cambridge, MA) and were killed at 1–60 d after injection as previously described (56, 63). After SDS-PAGE, radiolabeled proteins were detected by fluorography (38) or autoradiography.

Radiolabeling of Glial Cell Proteins of the Optic Pathway In Situ

Intact, unlabeled optic pathways, freshly dissected from mice, were incubated for 60 min at 37°C in 0.5 ml of a Hepes medium (25 mM Hepes, 5 mM KCl, 110 mM NaCl, 50 mM glucose, pH 7.4) containing 75 μCi of [^{35}S]methionine (sp act, 400 Ci/mmol). The medium was then replaced by 1.0 ml of the same medium without radioisotopic amino acid but containing protein synthesis inhibitors (0.5 mM cycloheximide [Sigma Chemical Co., St. Louis, MO] and 0.3 mg/ml chloramphenicol [Sigma Chemical Co.]). Incubation in this medium was continued at 37°C for an additional 5 min. This was repeated once to remove unincorporated radioactivity, and the tissue was then frozen at −70°C until analyzed (57).

Radioiodination of Proteins in Polyacrylamide Gel Slices

Protein bands to be radiolabeled were excised from Coomassie Blue-stained PAGE gels and washed extensively with 10% methanol over 3 d. The gel slices were lyophilized and then radiolabeled by the chloramine T procedure (15).

Two-dimensional α-Chymotryptic Peptide Map Analysis

Washed gel slices containing iodinated proteins were lyophilized and then incubated for 20 h at 37°C with 1.0 ml of 0.05 M NH_4HCO_3, pH 8.0, containing 10 μg of α-chymotrypsin. The digests were lyophilized, redissolved in 10–20 ml of Buffer I (acetic acid/formic acid/H_2O, 15:5:80), spotted onto cellulose-coated TLC plates, and subjected to electrophoresis in Buffer I at 1 kV for 30 min and then chromatographed in butanol/pyridine/acetic acid/H_2O (32.5:25:5:20) as described previously (15). The radioactive peptides were visualized by autoradiography.

Alkaline Phosphatase Digestion of Cytoskeletal Proteins

Cytoskeletal protein fractions were incubated at 37°C with *Escherichia coli* alkaline phosphatase (48 U/mg protein; Sigma Chemical Co., St. Louis, MO) in 0.05 M Tris containing 100 mM NaCl, 0.5 mM PMSF, 100 μg/ml leupeptin, and 0.1% aprotinin. After a 5-h incubation, the cytoskeletal proteins were pelleted by centrifugation and prepared for SDS-PAGE as previously described.

Immunostaining with Monoclonal and Polyclonal Antibodies

Optic pathway proteins on gels after SDS-PAGE were transformed onto nitrocellulose using 0.45-μm nitrocellulose membranes (Millipore Continental Water Systems, Bedford, MA). After transfer, unbound sites on the nitrocellulose were blocked for 1 h in 10% normal goat serum (Rockland, Inc., Gilbertsville, PA) in 50 mM Tris-HCl, pH 7.4, containing 0.9% NaCl and 0.1% aprotinin. Blocked membranes were stained by an indirect immunoperoxidase method using 3',3'-diaminobenzidine (Sigma Chemical Co.) as the peroxidase substrate (5). In some experiments, immunoblot analyses were carried out using ^{125}I-labeled rabbit anti-mouse IgG (New England Nuclear, Boston, MA) as the secondary antibody in the indirect immunochemical procedure. In this case, immunoreactive proteins on nitrocellulose papers were visualized by autoradiography. Antibodies used in this study included a polyclonal antiserum against phosphorylated epitopes on NF-H (obtained from Dr. R. Majocha) (7, 76), a monoclonal antibody (R3) against phosphorylated epitopes on NF-H (14) (obtained from Dr. U. Drager), and monoclonal antibodies against phosphorylated and unphosphorylated epitopes on NF-H (80), SMI 31 and 32, respectively (Sternberger-Meyer Immunocytochemicals, Inc., Jarrettsville, MD).

Quantitation of Unlabeled and Radiolabeled Proteins by Densitometry

The relative content of Coomassie-stained proteins on SDS gels was quantitated by densitometry. Enlarged photographs of the stained gels were printed on Mylar transparent sheets and scanned using an Ultroscan laser densitometer (LKB Instruments, Inc., Gaithersburg, MD). Densities of regions on the gel corresponding to individual NF-H variants were quantitated by integrating the area under the scanned region using a computer digitizing board interfaced with a Bioquant software program (R & M Biometrics, Inc., Nashville, TN). Corrections for background were made by subtracting the density of an equivalent region of gel containing no protein bands. For a given experiment, all scans were performed at the same settings to enable direct comparisons of relative protein content. All determinations were made at staining intensities that, in previous experiments, were observed to be in a range in which optical density was directly proportional to protein content. Radiolabeled proteins were similarly quantitated by densitometric analysis of autoradiograms or fluorograms of appropriate exposures. A background value was subtracted which was equivalent to the density of a region of the gel lane that contained no radioactive protein bands. In some experiments (e.g., Fig. 11), scans of all samples were normalized to one same total density (area under the curve). Scans from replicate samples were then averaged together after calculating the density at consecutive points along each normalized scan.

Results

Heterogeneity of 200-kD Proteins in Axons of Retinal Ganglion Cells

Mouse optic axons contain proteins with apparent molecular masses of 195–210, 140–145, and 70 kD, which have been identified by biochemical and physiological criteria (7, 63, 65) as NF-H, NF-M, and NF-L, respectively. Although unusual charge properties and extensive phosphorylation of the NF-M and NF-H subunits cause anomalous electrophoretic migration patterns that lead to overestimates of true molecular size (17, 31, 34), molecular mass determinations by SDS-PAGE will be used to denote individual protein forms in these studies.

On SDS gels containing a 5–15% acrylamide gradient, proteins in the 195–210-kD size range, referred to hereafter as the 200-kD proteins, appeared as a diffuse single band or doublet (Fig. 1, lane *b*). This region, however, could be resolved on 3–7% acrylamide gradient gels into four Coomassie Blue–stained bands displaying apparent molecular masses of 210, 205, 200, and 197 kD (Fig. 1, lane *a*). Since the patterns revealed by Coomassie Blue staining reflect the protein pools in optic glial cells as well as optic axons, we labeled proteins in optic axons selectively by injecting mice intravitreally with [^{35}S]methionine and analyzed them after 4 d (Fig. 1, lanes *c* and *d*). Four radiolabeled proteins (Fig. 1, lane *d*; Fig. 2, lanes *c* and *e*) were resolved that corresponded in electrophoretic migration to the four 200-kD proteins visualized by Coomassie Blue staining. For reasons discussed later, the level of radioactivity associated with the 210- and 197-kD proteins depended on the postinjection in-

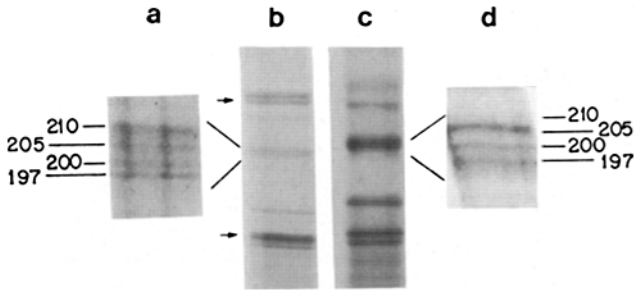

Figure 1. SDS-PAGE analysis of Coomassie Blue-stained optic nerve proteins (lanes *a* and *b*) and radiolabeled polypeptides in optic axons of mice 3 d after intravitreal injection of [^{35}S]methionine (lanes *c* and *d*). The region of the gels containing the 200-kD proteins is depicted. Top and bottom arrrows adjacent to lane *b* indicate the position of fodrin (235 kD) and NF-M (145 kD), respectively. The total protein content of optic axons, stained with Coomassie Brilliant Blue, is shown on gels containing polyacrylamide gradients of 3–7% (lane *a*) or 5–15% (lane *b*). ^{35}S-labeled proteins in optic axons, revealed by fluorography, are shown on gels containing polyacrylamide gradients of 5–15% (lane *c*) or 3–7% (lane *d*).

terval, but each of the four radiolabeled proteins was easily distinguished under certain conditions (Figs. 2, 5, and 6).

Since assembled neurofilaments are considered to be highly insoluble polymers (52), we screened for putative forms of the NF-H subunit by determining the solubilities of the four 200-kD proteins in Triton X-100 solutions. Proteins from optic nerves of mice injected intravitreally with [^{35}S]-methionine were partitioned into Triton-soluble and -insoluble fractions and analyzed by SDS-PAGE. Coomassie Blue staining of these gels indicated that the Triton-insoluble fraction contained all four 200-kD proteins (designated P210, P205, P200, P197) and that each was a major protein constituent of optic axons (Fig. 2, lane *a*; also Fig. 1, lane *a*). The Triton-soluble fraction, however, contained only a 197-kD protein (S197) in appreciable amounts (Fig. 2, lane *b*).

The composition of radiolabeled 200-kD proteins in these fractions resembled the pattern on stained gels although some differences were noted. P210, the most prominently stained 200-kD protein, was weakly radiolabeled at 2 d after injection (Fig. 2, lane *d*) but discerned clearly after longer postinjection intervals (Fig. 2, lane *e*; also see below). The Triton-soluble fraction contained prominent radiolabeled

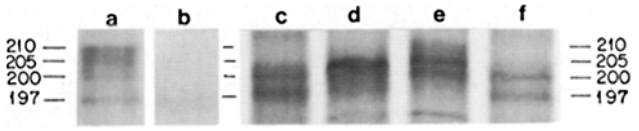

Figure 2. SDS-PAGE analysis of Triton-insoluble and Triton-soluble 200-kD proteins from unlabeled optic axons (lanes *a* and *b*) or optic axons obtained from mice 2 or 5 d after intravitreal injection of [^{35}S]methionine (lanes *c–f*, see below). Only the 200-kD region of the gels (3–7% polyacrylamide gradient) is depicted. Total protein content from Triton-insoluble fractions (122 μg protein loaded) (lane *a*) and Triton-soluble fractions (182 μg protein loaded) (lane *b*) of optic axons was revealed by staining with Coomassie Brilliant Blue. Radiolabeled proteins in optic axons at 2 d after injection (lane *c*, soluble; lane *d*, insoluble) or at 5 d after injection (lane *e*, insoluble; lane *f*, soluble) on adjacent lanes of the same gel were detected by fluorography. Labeled soluble fractions contained 91 μg of protein and insoluble fractions contained 61 μg of protein.

200-kD (S200) and 197-kD (S197) polypeptides (Fig. 2, lanes *c* and *f*) which were barely detectable by Coomassie Blue staining (Fig. 2, lane *b*). These results confirmed that retinal ganglion cells synthesize four Triton-insoluble and two Triton-soluble 200-kD proteins. Classification according to solubility properties proved to be an important criterion for identifying neurofilament proteins since the following data show that only the insoluble 200-kD proteins in optic axons exhibited properties expected of neurofilament subunits.

Structural Relatedness of 200-kD Proteins

To examine the structural homology among 200-kD proteins, the Triton-soluble and -insoluble forms of these polypeptides were excised from gels, iodinated with ^{125}I, and subjected to two-dimensional peptide map analysis after α-chymotrypsin digestion. Of the 34 peptides clearly discernible on the peptide map of P210, 33 were present in P205, 32 were shared by P200, and 30 were present in P197. The P205 and P200 proteins shared two to five additional peptides not detectable on the map of P210. In contrast to the high degree of structural homology among Triton-insoluble 200-kD proteins, only 10 of the peptides common to each of these polypeptides had possible counterparts on the maps of the Triton-soluble proteins (Fig. 4). An additional 22–40 peptides on maps of S200 and S197 were not shared by the insoluble 200-kD proteins. Considerable homology (70–80%) was observed, however, between the two Triton-soluble proteins (Fig. 4).

Differential Axoplasmic Transport of the 200-kD Proteins

Intravitreal injection of radiolabeled amino acids intensely labels the three neurofilament subunits, which then advance along optic axons in the slowest phase (Group V or SCa) of axoplasmic transport (0.3–0.7 mm/d) (3, 26, 62, 87, 89). To compare the transport characteristics of 200-kD proteins with these established patterns, we injected mice intravitreally with [^{3}H]proline and, after 3 or 7 d, divided the optic pathway into consecutive 1.1-mm segments (Fig. 5). These were then separated into Triton-soluble and -insoluble fractions, subjected to electrophoresis, and quantitated by laser densitometry after fluorography. Changes in the distribution of individual Triton-soluble and -insoluble proteins between 3 and 7 d (Fig. 5) demonstrated the progressive advance of these proteins along optic axons by axoplasmic transport as previously established (62, 63, 65). At 7 d after injection, the transport wave containing P210, P205, P200, and P197, which advanced at 0.3–0.5 mm/d, was clearly separated from the transport wave containing Triton-soluble 200-kD proteins, which advanced at a typical Group IV (SCb) rate (1–2 mm/d) based upon comparisons with other typical Group IV proteins (62). A small proportion of P205 protein also moved at a Group IV rate. An autoradiogram (Fig. 5, *inset*) depicting the labeling patterns of Triton-insoluble and -soluble 200-kD proteins in the optic nerve and optic tract at 5 d after isotope injection distinguished the P205 variant moving in Group IV from the other Triton-insoluble 200-kD proteins moving in Group V (Fig. 5, lanes *a* vs. *b*) and illustrates the appearance of S200 and S197 in the optic tract by 5 d (Fig. 5, lane *d*) as predicted from a Group IV transport rate (1 mm/day) (Fig. 5, lanes *c* vs. *d*).

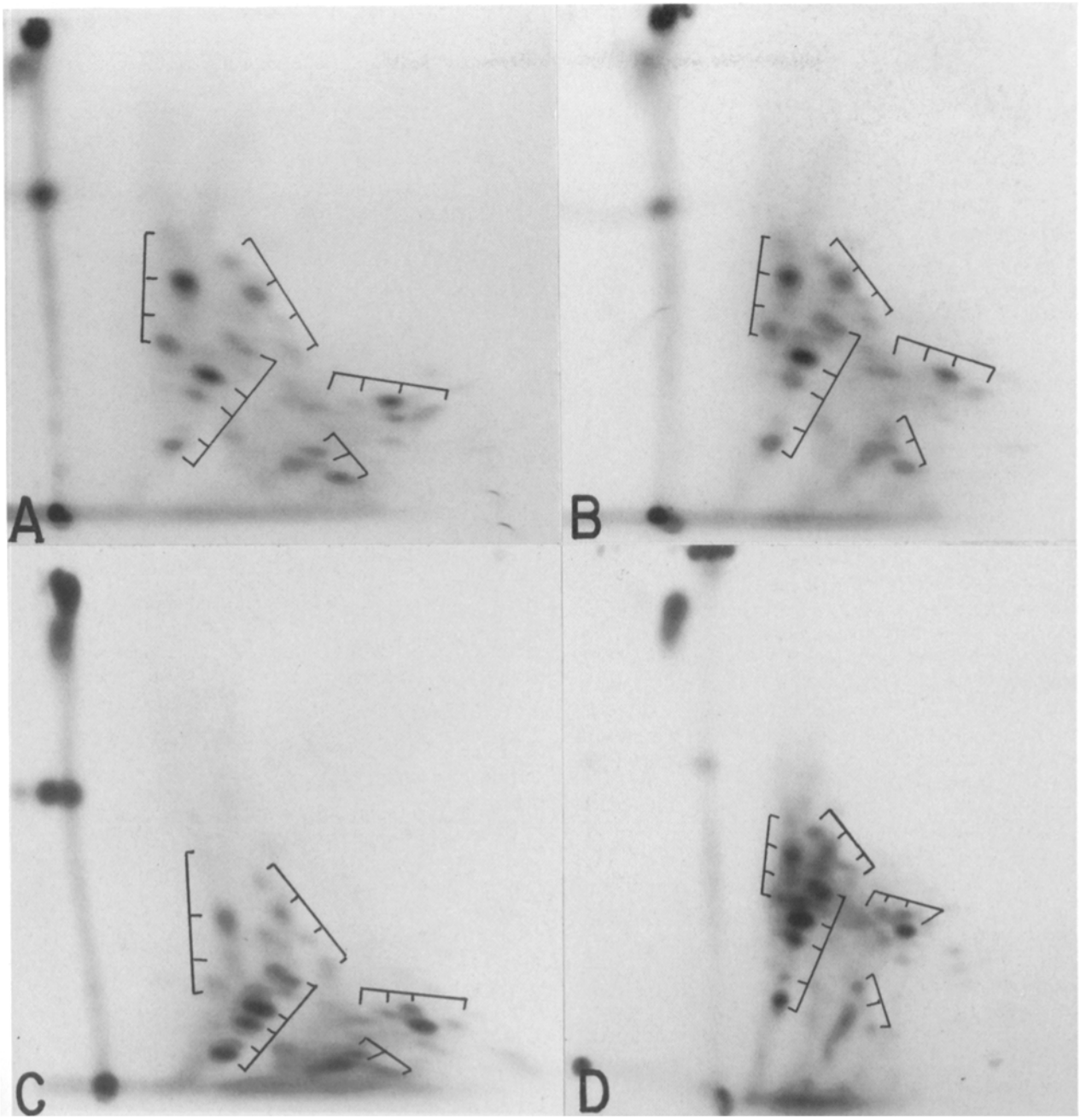

Figure 3. Two-dimensional peptide map analyses of Triton-insoluble 200-kD proteins from mouse optic axons. Each of the four Triton-insoluble individual 200-kD proteins was excised from SDS gels, iodinated with ^{125}I, and digested with α-chymotrypsin (see Materials and Methods). Chymotryptic peptides, separated in the first dimension (*left to right*) by high voltage electrophoresis and in the second dimension (*bottom to top*) by TLC, were revealed by autoradiography. Homologous configurations of peptides derived from P210, P205, P200, and P197 (*a–d*, respectively) are indicated on each peptide map.

Phosphorylation and Dephosphorylation of 200-kD Proteins

The subunits of all classes of intermediate filaments appear to contain phosphate (83). Intravitreal injection of [^{32}P]orthophosphate in mice has also been shown to label a limited group of axonal proteins, which includes the three neurofilament subunits (61, 65). Among the 200-kD proteins, only the Triton-insoluble group incorporated ^{32}P (Fig. 6, cf. lanes *a* and *b*). In separate experiments, glial proteins were radiolabeled in situ by incubating excised but otherwise intact optic nerves in the presence of [^{32}P]orthophosphate under conditions that preserve the cellular integrity of the tissue (Fig. 6, lanes *c* and *d*). Although numerous proteins including α-fodrin (Fig. 6, lane *c*) and myelin basic protein (not shown) were intensely labeled, no ^{32}P radioactivity was detected in the 197–210-kD region of gel lanes containing Triton-insoluble proteins (Fig. 6, lane *c*). Two Triton-soluble proteins in this region of the gel incorporated low levels of radioactivity (Fig. 6, lane *d*).

To obtain evidence for the in vivo phosphorylation of each of the four 200-kD proteins, we took advantage of a previous

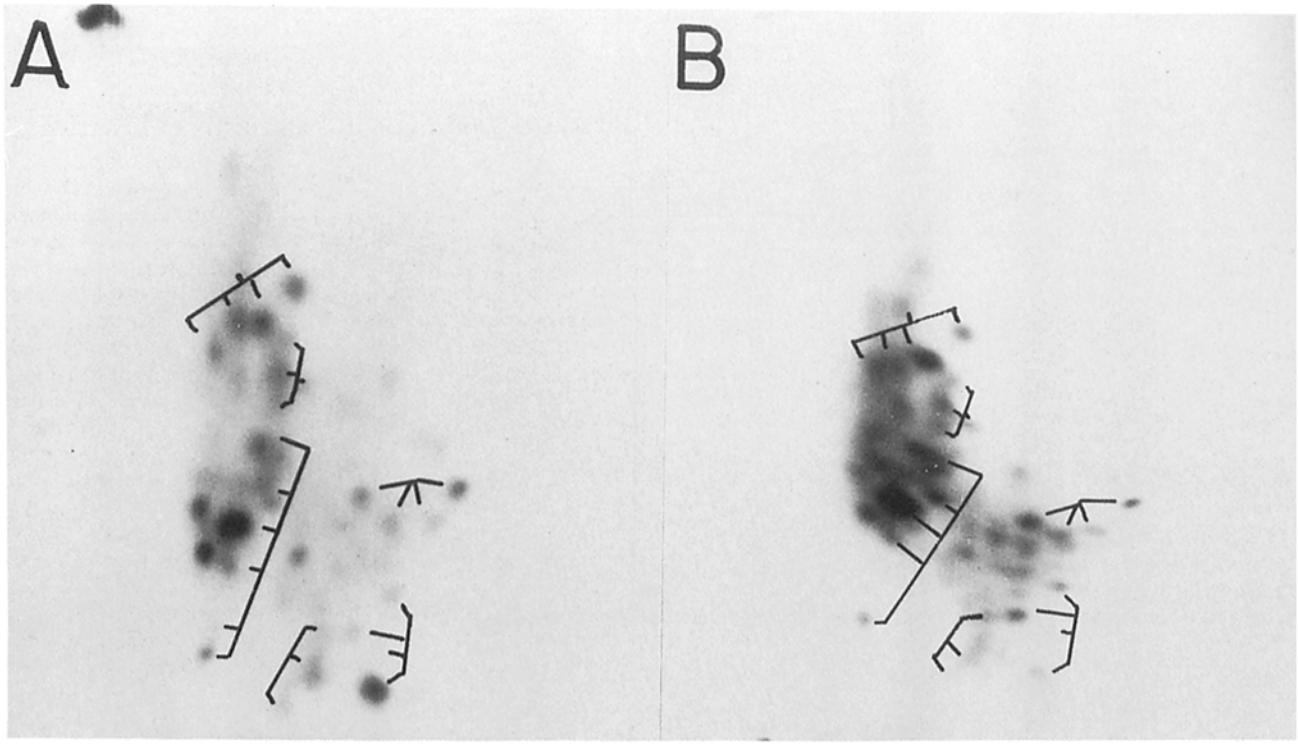

Figure 4. Two-dimensional peptide map analysis of Triton-soluble 200-kD axonal proteins. The α-chymotryptic peptide maps of the Triton-soluble 200-kD proteins S200 (*A*) and S197 (*B*) were prepared from mouse optic axons as described in Fig. 3. Autoradiograms show common configurations of peptides.

observation (Fig. 2) that P197 was more prominently radiolabeled at the earliest postinjection timepoint and P205 and P210 were most abundant at longer survival times (also see below). Autoradiograms of 200-kD proteins in optic axons from mice obtained 5 h after injection of [^{32}P]orthophosphate revealed ^{32}P radioactivity evenly distributed within the region of the SDS gel that included P197 and P200 (Fig. 6, lane *f*). By 5 d after injection, radiolabeled forms in optic nerve (Fig. 6, lane *g*) and optic tract (Fig. 6, lane *h*) comigrated predominantly in the region of P205 and P210 and included only small proportions of P200 and little, if any, P197. The conclusion that each of the Triton-insoluble 200-kD proteins incorporated ^{32}P in vivo, suggested by these distribution patterns, was further supported by immunochemical studies below.

Certain structural features of neurofilament subunits, including phosphorylation state, may be distinguished by the differential reactivity of the subunit with antibodies directed against specific peptide sequences or epitopes containing or lacking phosphate (80). Individual 200-kD proteins excised from 3–7% polyacrylamide SDS gels were placed in adjacent lanes of a second SDS gel and subjected to electrophoresis again. The proteins were electroblotted onto nitrocellulose and immunostained with NF-H monoclonal antibodies. The four Triton-insoluble polypeptides were detected by immunostaining the transferred proteins with a monoclonal antibody (SMI 32) that recognizes phosphatase-insensitive (presumably nonphosphorylated) epitopes on neurofilament proteins (Fig. 7 *A*) (80). SMI 31 (Fig. 7 *B*) (80) and R3 (data not shown) (14), two monoclonal antibodies that exclusively recognize phosphorylated epitopes, also immunostained these proteins. In addition, EL, an antiserum which is also specific for phosphorylated epitopes (76) recognized all four forms (Fig. 7 *C*). The 197-kD variant, however, reacted less strongly compared to the other proteins with SMI 31 but not with SMI 32 (Fig. 7 *B*). This differential staining pattern was reproducibly seen in multiple analyses. In contrast to these results, the Triton-soluble 200-kD polypeptides did not cross-react with these antibodies (Fig. 7, lanes *e* and *f*).

The majority of phosphate groups on NF-H can be removed in vitro by alkaline phosphatase treatment (8, 31, 65). We used this strategy to examine whether the Triton-insoluble 200-kD proteins were all phosphorylated or included a population of unphosphorylated NF-H variants. Axonal cytoskeletal proteins before and after incubation with *E. coli* alkaline phosphatase for 5 h at 37°C were compared by Coomassie Blue staining and immunoblot analysis using the SMI32 and SMI31 antibodies (Fig. 8). Dephosphorylation was associated with the complete disappearance of the four Triton-insoluble 200-kD proteins from their typical migration positions on gels (Fig. 8, lanes *a* and *c*) and appearance of a major immunoreactive protein at 160 kD (Fig. 8, lanes *b* and *d*), where newly synthesized unmodified NF-H subunits comigrate (18, 61, 69). The phosphorylated and dephosphorylated NF-H subunits displayed a high degree of structural homology when two-dimensional iodopeptide maps were analyzed after digestion with α-chymotrypsin: more than 95% of the major peptides were shared in common (Fig. 9).

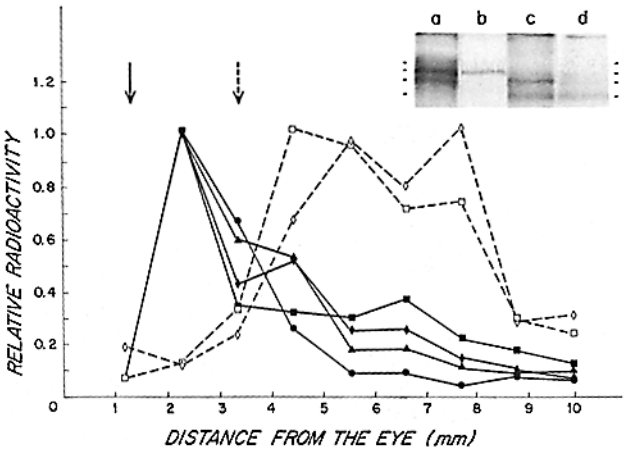

Figure 5. Comparison of axoplasmic transport distribution profiles for Triton-soluble and Triton-insoluble 200-kD proteins from mice 3 or 7 d after intravitreal injection of [^{3}H]proline. The optic nerves and proximal optic tracts of groups of 20 mice at each timepoint were divided into nine consecutive 1.1-mm segments, which were then separated into Triton-soluble and Triton-insoluble fractions and subjected to SDS-PAGE (3–7% polyacrylamide gradient). Radioactivity associated with the four Triton-insoluble 200-kD proteins (*solid lines*) P210 (●), P205 (■), P200 (▲), and P197 (◆), and two Triton-soluble 200-kD proteins (*dotted lines*), S200 (□) and S197 (◇), was determined on fluorograms by laser densitometry. The relative distribution of each radiolabeled polypeptide along optic axons at 7 d after injection is illustrated. The optic chiasm begins after segment 5. The peaks of the transport wave for the labeled Triton-insoluble proteins (*solid arrow*) and Triton-soluble proteins (*dotted arrow*) at 3 d after injection are indicated to illustrate the movement of the wave during this time interval. (*Inset*) Autoradiogram from a single SDS gel (3–7% polyacrylamide gradient) containing radiolabeled proteins in Triton-insoluble (lanes *a* and *b*) and Triton-soluble (lanes *c* and *d*) fractions of optic nerve (lanes *a* and *c*) and optic tract (lanes *b* and *d*) 5 d after mice were injected intravitreally with [^{35}S]methionine. Protein loads on gels are the same as those in Fig. 2.

Non-Uniform Distribution of 200-kD Proteins along Optic Axons

Neurofilaments are twice as numerous at distal levels of mouse optic axons than at proximal levels. To investigate the relationship of the individual Triton-insoluble 200-kD proteins (NF-H variants) to steady-state pools of neurofilaments, we examined the axonal distributions of these variants by measuring the total content of each variant in proximal, middle, and distal levels of the optic nerve and optic tract by laser densitometry after the proteins were separated by SDS-PAGE and stained with Coomassie Blue. The content of the 210- and 205-kD polypeptides, like that of NF-M and NF-L subunits, increased markedly from proximal to distal levels of optic axons (Fig. 10). The P200 variant, by contrast, displayed a relatively uniform distribution. Finally, P197 was the most prominent variant in proximal segments but was the least prominent variant at distal levels of optic axons (Fig. 10).

Association of 200-kD Proteins with the Stationary Neurofilament Network along Axons

Previous studies demonstrate that neurofilament proteins are associated with at least two types of neurofilaments in optic axons: those undergoing continuous slow axoplasmic transport and those that are stationary and comprise the predominant neurofilament network along optic axons (62). To seek differences in the association of individual Triton-insoluble

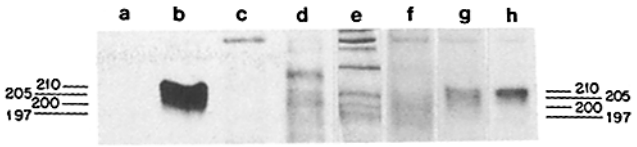

Figure 6. Autoradiograms of 200-kD proteins in optic axons of mice radiolabeled by intravitreal injection of [^{32}P]orthophosphate (lanes *a*, *b*, and *f–h*) or [^{35}S]methionine (lane *e*). Proteins in optic nerve glia were selectively labeled by [^{32}P]orthophosphate (lanes *c* and *d*) as described in Materials and Methods. Triton-soluble and -insoluble fractions of radiolabeled proteins in neurons (lanes *a* and *b*, respectively) and glia (lanes *d* and *c*, respectively) were analyzed by SDS-PAGE (3–7% polyacrylamide gradient) followed by autoradiography. Fractions from equivalent masses of labeled optic axons or optic glia are shown. Protein loads on gels are the same as those in Fig. 2. Lanes *e–h* depict autoradiograms of SDS gels containing 200-kD proteins from optic nerve 3 d after [^{35}S]methionine (lane *e*); optic nerve 5 h after [^{32}P]orthophosphate (lane *f*); optic nerve 5 d after [^{32}P]orthophosphate (lane *g*); optic tract 5 d after [^{32}P]orthophosphate (lane *h*). Lanes *e*, *g*, and *h* are taken from the same SDS gel. A second [^{35}S]methionine-labeled optic nerve (not shown), subjected to electrophoresis in the lane adjacent to lane *f*, enabled precise alignment of lane *f* with other lanes in this figure. Varying exposure times were used for autoradiograms of each lane to facilitate comparisons.

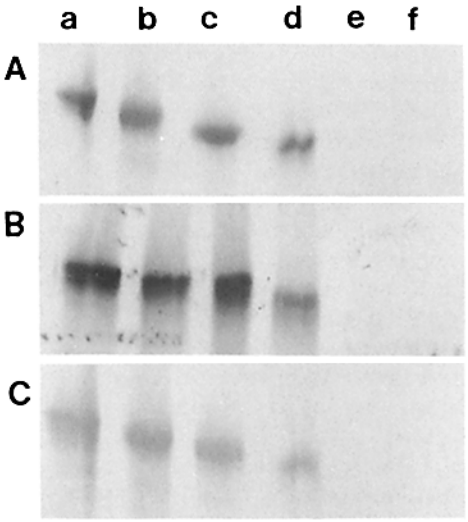

Figure 7. Immunoblot analysis of 200-kD proteins with anti-NF-H monoclonal antibodies directed against phosphatase-insensitive epitope(s) (SMI 32; *A*) or phosphatase-sensitive epitope(s) (SMI 31; *B*), and a polyclonal antiserum directed against phosphatase-sensitive epitope(s) on NF-H (7, 76) (EL; *C*). Triton-insoluble proteins from optic axons were separated by SDS-PAGE (3–7% polyacrylamide gradient). Individual bands corresponding to the four Triton-insoluble proteins P210 (lane *a*), P205 (lane *b*), P200 (lane *c*), and P197 (lane *d*), and two Triton-soluble proteins, S200 (lane *e*) and S197 (lane *f*), were separated by SDS-PAGE (3–7% polyacrylamide gradient), excised from the gel, subjected again to electrophoresis in adjacent lanes of a second gel, and then subjected to Western blot analysis. An amount of each polypeptide derived from an equivalent amount of fresh tissue (4 mg) was loaded into each lane.

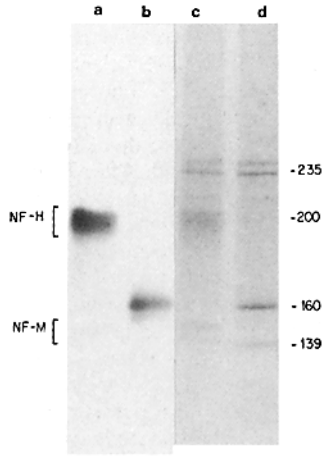

Figure 8. SDS-PAGE analysis of NF-H subunits before and after neurofilaments in Triton-insoluble fractions of optic axons were dephosphorylated by incubation for 5 h in vitro with *E. coli* alkaline phosphatase. A combination of SMI 31 and SMI 32 antibodies was used in Western blot analysis to detect NF-H before (lane *a*) or after (lane *b*) dephosphorylation. Equal amounts of protein (120 μg) were applied to each lane. For comparison, the same SDS gel, after electroblotting, was stained with Coomassie Blue to demonstrate the remaining protein corresponding to NF-H before (lane *c*) and after (lane *d*) dephosphorylation.

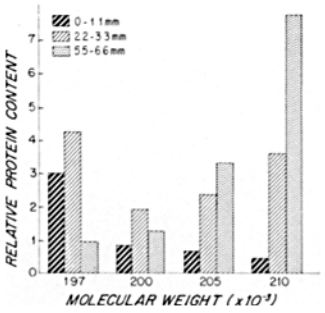

Figure 10. Axonal distribution of the four NF-H variants P210, P205, P200, and P197, at distances 0–1.1, 2.2–3.3, and 5.5–6.6 mm from the eye as indicated on the graph. Triton-insoluble fractions were prepared from each of these sets of 1.1-mm segments of the optic pathway pooled from 20 mice. After SDS-PAGE (3–7% polyacrylamide gradient), the regions of the Coomassie Blue–stained gel corresponding to each of the four NF-H variants were analyzed by laser densitometry and the total protein content, expressed in arbitrary units, was plotted.

200-kD proteins (NF-H variants) with these two types of neurofilaments, we compared the proportions of each radiolabeled variant as radiolabeled neurofilament proteins were initially entering axons in the advancing wavefront of slow axoplasmic transport and at stages during and after the integration of transported neurofilaments into the stationary cytoskeleton (Fig. 11). Mice injected intravitreally with [^{35}S]-methionine were analyzed at timepoints when (*a*) labeled neurofilaments were predominantly in a moving phase (3 d), (*b*) both moving and stationary neurofilaments were well radiolabeled (15 d), or (*c*) labeled stationary neurofilaments predominated along optic axons (60 d). These timepoints were based on the results of previous studies (62). The optic axon segments, dissected from mice at these three timepoints, were fractionated and the Triton-insoluble fraction was analyzed by SDS-PAGE. Densitometric scans of the autoradiographs from multiple gels demonstrated that, at 3 d after injection, polypeptides migrating within the 195–205-kD region of the gel were the most intensely labeled NF-H variants (Fig. 11). By 60 d after injection, labeling in the 195–197-kD region was markedly diminished; however, P210 was intensely labeled, and P205 also displayed increased radioactivity. At the 15-d postinjection timepoint, when both moving and stationary neurofilaments were radiolabeled, the radioactivity displayed a pattern intermediate between the 3- and 60-d timepoints.

Discussion

Multiple Structural Variants of NF-H in Axons

In this study, we have identified a set of four 197–210-kD polypeptides as variants of the NF-H subunit of neurofilaments. The property of Triton X-100 insolubility, a previously established characteristic of axonal neurofilaments (51), effectively distinguished all neurofilament-related 200-

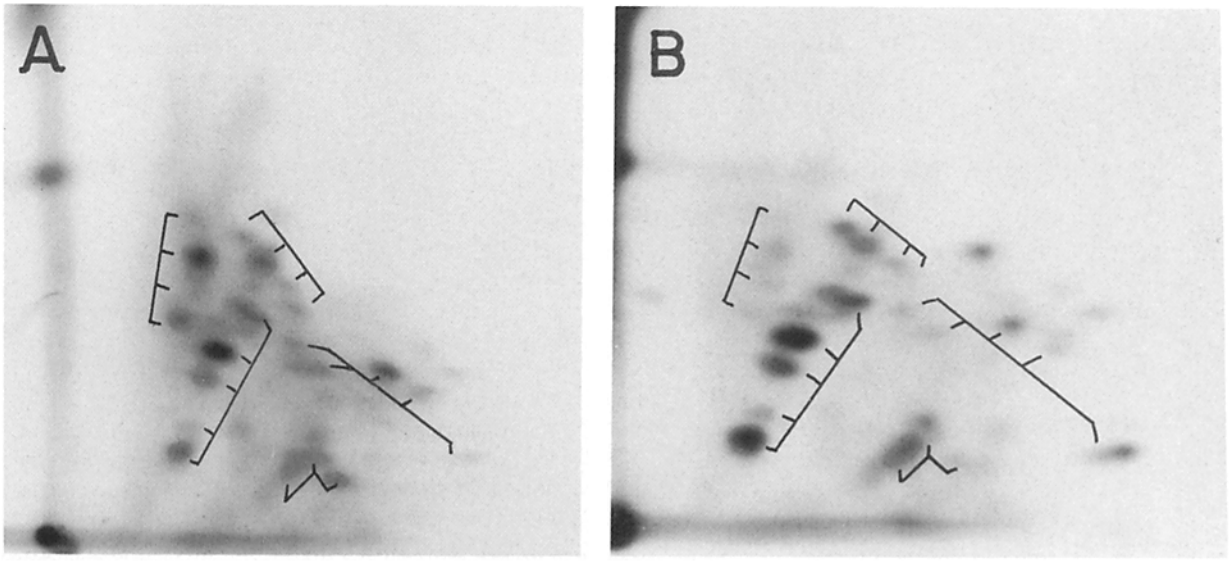

Figure 9. Two-dimensional peptide map analysis of NF-H subunits before (*A*) and after (*B*) neurofilaments were dephosphorylated by incubation for 5 h in vitro with *E. coli* alkaline phosphatase. Iodopeptide map analysis after α-chymotrypsin digestion was performed as described in Fig. 3. Homologous configurations of peptides are indicated.

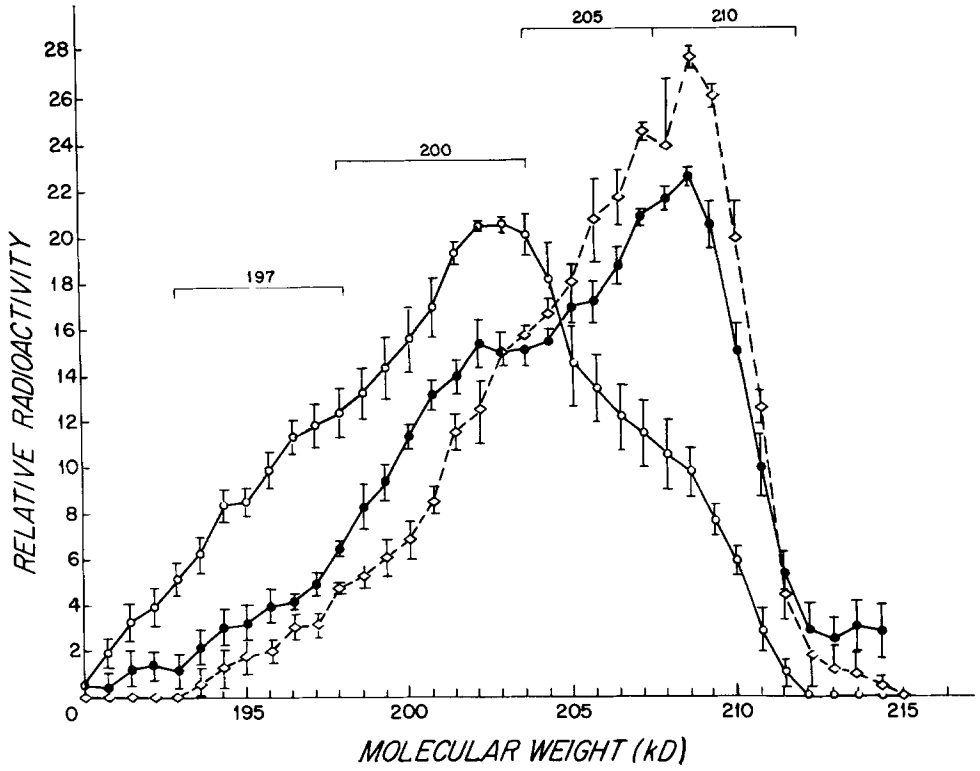

Figure 11. Relative proportions of radiolabeled NF-H variants present in optic axons from mice injected intravitreally with [^{35}S]methionine and killed after 3 (○), 15 (●), and 60 (◇) d. After Triton-insoluble proteins were separated by SDS-PAGE, the relative radioactivity of individual NF-H variants was determined on autoradiograms by laser densitometry. Since the absolute radioactivity of NF-H varied at the different postinjection timepoints, the different scans were normalized to the same total radioactivity; i.e., area under the scan. Each data point represents the mean ± SEM for three to four separate experiments. The approximate locations along the scan corresponding to each NF-H variant are provided at the top of the figure.

kD proteins in optic axons from unrelated proteins with similar apparent molecular masses. Each of the four Triton-insoluble 200-kD proteins was synthesized in neurons (Figs. 1 and 2), advanced along axons predominantly or exclusively in the Group V (SCa) phase of axoplasmic transport (3, 89) (Fig. 5), and incorporated phosphate groups in vivo (30) (Fig. 6). In addition, each of the four proteins cross-reacted with antibodies to an epitope common to all classes of intermediate filament proteins (72) (data not shown) and with a set of monoclonal and polyclonal antibodies against NF-H (Fig. 7). Finally, the four polypeptides displayed more than 90% homology by two-dimensional peptide map analysis after α-chymotryptic digestion (Fig. 3). The extremely close structural homology between these NF-H variants suggests that relatively small modifications that influence the charge or conformation of the protein accounted for apparent molecular mass differences on SDS gels. Although closely related, the individual NF-H variants could be clearly distinguished from each other by differences in their electrophoretic mobilities, their relative specific radioactivities at different times after pulse-labeling with [^{35}S]methionine in vivo, and their regional distribution along axons.

Two Triton-soluble 200-kD proteins, by contrast, satisfied few if any conventional criteria for neurofilament protein identification. Although they displayed apparent molecular masses roughly similar to those of certain NF-H variants, they were transported more rapidly than neurofilament proteins Group IV or SCb transport phase (Fig. 5), did not incorporate phosphate in vivo (Fig. 6), and were not recognized by antibodies to NF-H (Fig. 7) or to the general class of intermediate filaments (72). They displayed some structural similarities to each other but only limited peptide homology with the NF-H variants (Fig. 4). Despite some structural similarities with NF-H, the Triton-soluble 200-kD proteins do not represent nonphosphorylated forms of NF-H, since unmodified NF-H subunits, as well as enzymatically dephosphorylated NF-H subunits, display an apparent molecular mass of 160 kD and retain more than 90% of peptide homology with extensively modified, insoluble forms of NF-H (Fig. 9). The high degree of homology between iodopeptide maps of phosphorylated and dephosphorylated forms of NF-H is not unexpected since many of the phosphate-rich chymotryptic peptides are unlabeled or weakly labeled by ^{125}I (Sihag, R. K., and R. A. Nixon, unpublished observations), suggesting, therefore, that they either lack iodination sites or that phosphorylation blocks iodination of potential sites on these peptides. It is also difficult to account for S200 and S197 as soluble proteolytic derivatives of NF-H variants since they contained no label after [^{32}P]orthophosphate administration. The heavily phosphorylated region of NF-H is at least 65 kD in size (16), and its removal should result in large molecular mass changes. This conclusion is further supported by the observation that each of the Triton-soluble proteins displays many α-chymotrypsin peptides that are not shared by any of the NF-H variants (Fig. 4).

One or both of the 200-kD soluble polypeptides may correspond to brain myosin (48), which migrated to an apparent molecular mass in the 197–200-kD range (Lewis, S. E., and R. A. Nixon, unpublished observations). In addition, we have observed that several [^{35}S]methionine-labeled axonal polypeptides with similar apparent molecular masses coassemble with microtubules, suggesting that one or both may be microtubule-associated proteins (Nixon, R. A., and I. Fischer, unpublished observations). A group of similarly sized microtubule-associated proteins has been observed in rat liver (35).

Microheterogeneous Variants of NF-H Are Phosphoproteins

Previous studies suggest several possible mechanisms to account for NF-H microheterogeneity, which was initially noted in early two-dimensional gel analyses of axonal neurofilament proteins (5, 12). The existence in rabbits of two NF-H isoforms differing in apparent molecular mass by 10,000 D is attributed to genetic polymorphism (86, 87). This phenomenon has not been observed in other species, including mice. Other examples of neurofilament protein microheterogeneity reflect modifications to the protein after it is synthesized. Limited proteolysis during axoplasmic transport, for example, generates major NF-M variants of lower apparent molecular mass that display a non-uniform distribution along optic axons (63, 67). These limited proteolytic modifications of NF-M within axons are distinct from the degradation of neurofilament polypeptides that reach nerve terminals (37, 58). In similar extensive studies of NF-H, we were unable to demonstrate interconversion of NF-H variants by limited proteolysis in vivo or in vitro (Lewis, S. E., and R. A. Nixon, unpublished observations).

Neurofilament protein microheterogeneity is also generated by protein phosphorylation (4, 18, 20, 30, 41, 69, 80) and dephosphorylation (60). The immunocytochemical detection of phosphorylated neurofilaments predominantly in axons and relatively less phosphorylated or unmodified subunits in neuronal perikarya (2, 41, 42, 80) has been corroborated by biochemical studies showing that newly synthesized NF-H and NF-M are extensively phosphorylated as they enter axons (1, 4, 18, 61). These previous studies of various neuron types have identified two NF-H variants, a relatively unmodified (160-kD) form predominating in perikarya and a phosphorylated (200-kD) form present in axons. The possibility that neurons contain multiple phosphorylated NF-H variants as major constituents of the axonal neurofilament lattice, however, was suggested by observations that each of the individual triplet proteins continues to undergo unique sequences of phosphorylation and dephosphorylation events during axoplasmic transport (60, 65).

Several lines of evidence indicate that microheterogeneity of NF-H subunit structure in optic axons arises by phosphorylation, and possibly dephosphorylation, during axonal transport. NF-H, the most highly phosphorylated subunit, contains between 25 and 50 phosphate groups per molecule (8, 29, 30). Since phosphate addition slows the electrophoretic mobility of many proteins (55), including NF-H (30, 34), varying phosphorylation states can easily account for differences in apparent molecular masses of the NF-H variants. When neurofilaments from mouse optic axons were enzymatically dephosphorylated, the four NF-H variants disappeared, giving rise to a 160-kD polypeptide (Fig. 8). This extensively dephosphorylated form comigrates on SDS gels with newly synthesized (unmodified) NF-H subunits labeled in vivo (61). These observations suggest that the varying molecular masses of the NF-H variants do not reflect size differences but, rather, changes in the electrophoretic mobility of the polypeptide induced by phosphate addition (34). Although it is conceivable that the varying electrophoretic mobilities of NF-H isoforms could reflect different conformational states of identically phosphorylated molecules, other data suggest that NF-H variants differ in net phosphorylation state. Previous studies indicate that phosphorylated NF-H subunits with the slowest electrophoretic mobility on SDS gels display a more acidic charge by IEF than subunits with a faster mobility (20, 82). Furthermore, the conversion of NF-H variants from lower to higher apparent molecular masses during axonal transport in optic axons (Figs. 2 and 6) is associated with a shift in isoelectric point of the NF-H subunit pool toward more acidic pH values, which is consistent with phosphate addition (65).

Available evidence suggests that phosphorylation may serve as a mechanism for coordinating the interactions of neurofilaments with other cytoskeletal elements during axoplasmic transport (65, 68). Neurofilament protein phosphorylation is a dynamic process involving multiple protein kinases (32, 33, 43, 77) and phosphatases (60). Not only do neurofilaments continue to be phosphorylated as they are transported along axons (65) but initially incorporated phosphate groups are also turned over with a specific timing and dependence on location within the axon (60). The rate of phosphate turnover is different for each of the neurofilament triplet proteins (60), and phosphates are removed preferentially from specific sites on at least the NF-L and NF-M subunits. Kinase and phosphatase systems involved in neurofilament phosphorylation, therefore, have the diversity and apparent specificity required of a mechanism for regulating complex protein–protein interactions. In addition to these observations, it is known that phosphates are primarily added to the carboxy-terminal tailpiece of NF-H which protrudes from the neurofilament core and presumably interacts with other cytoskeletal proteins (8, 16, 32). Electron microscopic studies (25, 75, 88) support the function of the peripheral domain of NF-H, in particular, as a cross-link between neurofilaments and microtubules. Other cytoskeletal proteins that may link intermediate filaments with microtubules or with the plasma membrane have also been shown to be phosphoproteins (55). For some of these proteins, phosphate addition to or removal from specific sites on the polypeptide markedly changes its binding affinities (23, 28, 47, 53, 73, 74).

Functional Implications of NF-H Microheterogeneity

The presence of multiple NF-H variants within axons of a single class of central neurons raises the possibility that these isoforms serve different functions. The suspected role of the NF-H subunits in forming cross-links between cytoskeletal elements (24, 25, 75, 88) is an additional reason to view the structural diversity of NF-H in functional terms. NF-H subunits form 4–6-nm-diam and 20–60-nm-long cross-bridges that link neurofilaments to other neurofilaments and possibly to microtubules and membrane-bound organelles (24). In addition, cross-bridges of different dimensions have been observed between neurofilaments and other organelles (24) although the participation of NF-H has not been firmly established. In developing neurons, the late appearance of phosphorylated forms of NF-H, after that of NF-L and NF-M (13, 71, 87), coincides with the transition from a state in which few interneurofilamentous cross-bridges exist to one in which most axonal neurofilaments are extensively cross-linked. This major reorganizational event during development may reflect changes in the functional state of the neurofilamentous cytoskeleton.

Mature retinal ganglion cell neurons contain two distinct axonal pools of neurofilaments which may have different functions (62). One pool, which is conveyed along axons in

the slowest phase of axoplasmic transport (Group V or SCa), displays a half-life of 17–20 d. These axonally transported neurofilaments contribute to a second, larger population that is stationary and forms a non-uniform neurofilament network along axons. This network, together with other stationary cytoskeletal elements (62), comprises a complex that turns over with a relatively long half-life (~55 d) (62). We have proposed that moving neurofilaments, unassociated or weakly associated with other cytoskeletal proteins, represent a relatively rapid mechanism for modifying axonal geometry to effect, for example, moderate changes in axonal caliber (27) or to repair local injury (58). While providing structural support, moving neurofilaments could also allow the degree of plasticity required by, for example, a growing axon during development. By contrast, the stationary neurofilament lattice in mature neurons is well suited as a framework to stabilize a given axonal shape, direction, or spatial orientation, and to organize and anchor constituents within the axoplasm (61, 62).

Our results provide evidence for a differential association of NF-H variants with the moving and stationary neurofilaments networks in optic axons. The 210- and 205-kD variants were observed to be major NF-H constituents of the stationary neurofilamentous cytoskeleton. These NF-H variants appear to arise from one or more of the lower molecular mass variants during axoplasmic transport since a shift from predominantly 197–205-kD forms at 3 d after pulse-radiolabeling (e.g., Figs. 2 and 11) to predominantly 205–210-kD forms at 15 d (Fig. 11) occurs without a significant decrease in total NF-H radioactivity (62). This conversion accords with previous observations that the phosphorylation state of NF-H increases during this time interval as axoplasmic transport proceeds (65). The 197-kD NF-H variant, by contrast, appears to be predominantly associated with the population of moving neurofilaments. This polypeptide was the principal NF-H form entering optic axons within 3 to 48 h after pulse-labeling in vivo (Figs. 6 and 11), and transport kinetics indicate that most neurofilaments at very proximal levels of optic axons are moving (62). Estimates of the total content of the four NF-H variants along axons (Fig. 10), in addition to showing that each is a major axonal protein, further support the distinction between neurofilaments predominantly composed of 197-kD NF-H subunits and those containing the 205- and 210-kD NF-H forms. The proximal to distal increase in P210 and P205 content along optic axons parallels the non-uniform deposition of neurofilaments containing radiolabeled P210 and P205 variants into the stationary cytoskeleton (62). If P197 were associated primarily with moving neurofilaments, its steady-state level along axons can only be expected to diminish proximally to distally, as we observed, when moving neurofilaments containing P197 variants become stationary neurofilaments containing P205 and P210 variants. Finally, P200 was a component of radiolabeled neurofilaments entering optic axons and those remaining in optic axons at 60 d after [^{35}S]methionine injection. The smaller proximal to distal differences observed in the content of this variant along axons are, therefore, consistent with its apparent association with moving and stationary neurofilaments.

Changes in the phosphorylation state of NF-H, reflected by the relative proportions of each NF-H variant, could, in fact, be viewed as a mechanism to regulate partitioning of neurofilaments between the moving and stationary neurofilament network. An analogy may be drawn to previously observed effects of phosphorylation on myosin structure (11). In the unphosphorylated state, myosin head domains are held down in the myosin filament backbone by head–head or head–backbone interactions. Phosphorylation inhibits these interactions causing the head domains to extend outward, which thereby facilitates cross-bridge formation with actin. By analogy, relatively dephosphorylated carboxyl-terminal domains of NF-H (and possibly NF-M) would be expected to have increased affinity for the filament core and to effect, therefore, a conformation of the neurofilament that is sterically favorable for its entry into the axon and its initial transport. Indeed, neurofilaments in some neurons appear to move at faster rates as they initially enter axons than when they reach more distal levels of the axon. Progressive phosphorylation of the carboxy-terminal domains of NF-M and NF-H would reduce interaction with the filament core, and the resulting radial extension of these domains would be expected to retard neurofilament movement and favor interactions with axonal elements, including constituents of the stationary cytoskeleton. Different conformations of the carboxy-terminal domains, represented by the different NF-H variants, might, therefore, define certain properties of the cross-bridges such as the spacing, reversibility, and specificity for moving or stationary elements.

Functional distinctions among different NF-H isoforms are further suggested by immunoblot analyses with a monoclonal antibody that recognizes a phosphatase-sensitive epitope on NF-H (2, 13). This antibody has been previously shown to immunostain axons only late in neuron development, considerably after the NF-H polypeptide appears and undergoes a certain degree of posttranslational modification by phosphate (2, 13). We have observed that this antibody recognizes the 210- and 205-kD NF-H variants and to a much lesser extent recognizes the 200 kD NF-H variant, but does not immunostain the 197-kD form (Nixon, R. A., S. E. Lewis, and D. Dahl, unpublished observations). Thus, the same NF-H variants that are distinguished by their differential associations with moving and stationary neurofilament networks appear also to be distinguished by the timing of their appearance during development.

We thank Drs. Ram Sihag and Thomas Shea and Ms. Kimberly Logvinenko for helpful discussions, and Mrs. Johanne Khan for assistance in preparing and typing the manuscript. We are also grateful to Dr. Ram Sihag for carrying out the two-dimensional peptide map analysis in Fig. 9, to Dr. Ursula Drager for providing the R3 antibody, and to Dr. Ronald Majocha for the gift of EL antiserum.

This research was supported by grants from the National Institute on Aging (AG 02126 and AG 05604).

Received for publication 17 June 1988, and in revised form 2 September 1988.

References

1. Bennett, G. S., and C. DiLullo. 1985. Slow posttranslational modification of a neurofilament protein. *J. Cell Biol.* 100:1799–1804.
2. Bignami, A., and D. Dahl. 1987. Axonal maturation in development. II. Immunofluorescence study of rat spinal cord and cerebellum with axon-specific neurofilament antibodies. *Int. J. Dev. Neurosci.* 5:29–37.
3. Black, M. M., and R. J. Lasek. 1980. Slow components of axonal transport: two cytoskeletal networks. *J. Cell Biol.* 86:606–623.
4. Black, M. M., P. Keyser, and E. Sobel. 1986. Interval between the synthe-

sis and assembly of cytoskeletal proteins in cultured neurons. *J. Neurosci.* 6:1004–1012.
5. Brown, B. A., R. A. Nixon, P. Strocchi, and C. A. Marotta. 1981. Characterization and comparison of neurofilament proteins from rat and mouse CNS. *J. Neurochem.* 36:143–153.
6. Brown, B. A., R. A. Nixon, and C. A. Marotta. 1982. Posttranslational processing of α-tubulin during axoplasmic transport in CNS axons. *J. Cell Biol.* 94:159–164.
7. Brown, B. A., R. E. Majocha, D. M. Staton, and C. A. Marotta. 1983. Axonal polypeptides cross-reactive with antibodies to neurofilament proteins. *J. Neurochem.* 49:299–308.
8. Carden, M. J., W. W. Schlaepfer, and V. M.-Y. Lee. 1985. The structure, biochemical properties, and immunogenicity of neurofilament peripheral regions are determined by phosphorylation state. *J. Biol. Chem.* 260: 9805–9817.
9. Chiu, F.-C., and W. T. Norton. 1982. Bulk preparation of CNS cytoskeleton and the separation of individual neurofilament proteins by gel filtration: dye-binding characteristics and amino acid compositions. *J. Neurochem.* 39:1252–1260.
10. Cleveland, D. V. 1983. The tubulins: from DNA to RNA to proteins and back again. *Cell.* 34:330–332.
11. Craig, R., R. Padron, and J. Kendrick-Jones. 1987. Structural changes accompanying phosphorylation of tarantula muscle myosin filaments. *J. Cell Biol.* 105:1319–1327.
12. Czosnek, H., D. Soifer, and H. M. Wisniewski. 1983. Studies on the biosynthesis of neurofilament proteins. *J. Cell Biol.* 85:726–734.
13. Dahl, D., C. J. Crosby, E. E. Gardner, and A. Bignami. 1986. Delayed phosphorylation of the largest neurofilament protein in rat optic nerve development. *J. Neurosci. Res.* 15:513–519.
14. Drager, U. C., D. L. Edwards, and C. J. Barnstable. 1984. Antibodies against filamentous components in discrete cell types of the mouse retina. *J. Neurosci.* 4:2025–2042.
15. Elder, J. H., R. A. Pickett, J. Hampton, and R. A. Lerner. 1977. Radioiodination of proteins in single polyacrylamide gel slices. *J. Biol. Chem.* 252:6510–6515.
16. Geisler, N., S. Fischer, J. Vanderkerckhove, J. Van Damme, U. Plessman, and K. Weber. 1985. Protein-chemical characterization of NF-H, the largest mammalian neurofilament component: intermediate filament-type sequences followed by a unique carboxy-terminal extension. *EMBO (Eur. Mol. Biol. Organ.) J.* 45:57–63.
17. Georges, E., and W. E. Mushynski. 1987. Chemical modification of charged amino acid moieties alters the electrophoretic mobilities of neurofilament subunits on SDS/polyacrylamide gels. *Eur. J. Biochem.* 165:281–287.
18. Glicksman, M. A., D. Soppet, and M. B. Willard. 1987. Posttranslational modification of neurofilament polypeptides in rabbit retina. *J. Neurobiol.* 18:167–196.
19. Goldstein, M. E., L. A. Sternberger, and N. H. Sternberger. 1983. Microheterogeneity ("neurotypy") of neurofilament proteins. *Proc. Natl. Acad. Sci. USA.* 80:3101–3105.
20. Goldstein, M. E., L. A. Sternberger, and N. H. Sternberger. 1987. Varying degrees of phosphorylation determine microheterogeneity of the heavy neurofilament polypeptide (NF-H). *J. Neuroimmunol.* 14:135–148.
21. Deleted in proof.
22. Granger, B. L., and E. Lazarides. 1985. Appearance of new variants of membrane skeletal protein 4.1 during terminal differentiation of avian erythroid and lenticular cells. *Nature (Lond.).* 313:238–241.
23. Herrman, H., J. M. Dalton, and G. Wiche. 1985. Microheterogeneity of microtubule-associated proteins, MAP-1 and MAP-2, and differential phosphorylation of individual subcomponents. *J. Biol. Chem.* 9:5797–5803.
24. Hirokawa, N. 1982. Cross-linker system between neurofilaments, microtubules, and membranous organelles in frog axons revealed by the quick-freeze, deep-etching method. *J. Cell Biol.* 94:129–142.
25. Hirokawa, N., M. A. Glicksman, and M. B. Willard. 1984. Organization of mammlian neurofilament polypeptides within the neuronal cytoskeleton. *J. Cell Biol.* 98:1523–1536.
26. Hoffman, P. N., and R. J. Lasek. 1975. The slow component of axonal transport. Identification of major structural polypeptides of the axon and their generality among mammalian neurons. *J. Cell Biol.* 66:351–366.
27. Hoffman, P. N., J. W. Griffin, and D. L. Price. 1984. Control of axonal caliber of neurofilament transport. *J. Cell Biol.* 99:705–714.
28. Huttner, W. B., W. Schiebler, P. Greengard, and P. de Camilli. 1983. Synapsin (protein I), a nerve terminal-specific phosphoprotein. III. Its association with synaptic vesicles studied in a highly purified synaptic vesicle preparation. *J. Cell Biol.* 96:1374–1388.
29. Jones, S. M., and R. C. Williams, Jr. 1982. Phosphate content of mammalian neurofilaments. *J. Biol. Chem.* 257:9902–9905.
30. Julien, J.-P., and W. E. Mushynski. 1981. A comparison of *in vitro* and *in vivo*-phosphorylated neurofilament polypeptides. *J. Neurochem.* 37: 1579–1585.
31. Julien, J.-P., and W. E. Mushynski. 1982. Multiple phosphorylation sites in mammalian neurofilament polypeptides. *J. Biol. Chem.* 257:10467–10470.
32. Julien, J.-P., and W. E. Mushynski. 1983. The distribution of phosphorylation sites among identified proteolytic fragments of mammalian neurofilaments. *J. Biol. Chem.* 258:4019–4025.
33. Julien, J.-P., G. D. Smoluk, and W. E. Mushynski. 1983. Characteristics of the protein kinase activity associated with rat neurofilament preparations. *Biochim. Biophys. Acta.* 755:25–31.
34. Kaufmann, E., N. Geisler, and K. Weber. 1984. SDS-PAGE strongly overestimates the molecular masses of the neurofilament proteins. *FEBS (Fed. Eur. Biochem. Soc.) Lett.* 170:81–84.
35. Kotani, S., H. Murofushi, S. Maekawa, H. Aizawa, and H. Sakai. 1988. Isolation of rat liver microtubule-associated proteins. Evidence for a family of microtubule-associated proteins with molecular mass of around 200,000 which distribute widely among mammalian cells. *J. Biol. Chem.* 263:5385–5389.
36. Laemmli, U. K. 1970. Cleavage of structural proteins during the assembly of the head of bacteriophage T4. *Nature (Lond.).* 227:685.
37. Lasek, R. J., and P. N. Hoffman. 1976. The neuronal cytoskeleton, axonal transport, and axonal growth. Microtubules and Related Proteins. *Cell Motil.* 3:1021–1049.
38. Laskey, R. A., and A. D. Mills. 1975. Quantitative film detection of ^{3}H and ^{14}C in polyacrylamide gels by fluorography. *Eur. J. Biochem.* 56:335–341.
39. Lazarides, E. 1982. Intermediate filaments: a chemically heterogeneous, developmentally regulated class of proteins. *Annu. Rev. Biochem.* 51: 219–250.
40. Lazarides, E., and W. J. Nelson. 1983. Erythrocytes and brain forms of spectrin in cerebellum: distinct membrane-cytoskeleton domains in neurons. *Science (Wash. DC).* 220:1295–1296.
41. Lee, V. M.-Y., M. J. Carden, and J. Q. Trojanowski. 1986. Novel monoclonal antibodies provide evidence for the *in situ* existence of a non-phosphorylated form of the largest neurofilament subunit. *J. Neurosci.* 6:850–860.
42. Lee, V. M.-Y., M. J. Carden, W. W. Schlaepfer, and J. Q. Trojanowski. 1987. Monoclonal antibodies distinguish several differentially phosphorylated states of the two largest rat neurofilament subunits (NF-H and NF-M) and demonstrate their existence in the normal nervous system of adult rats. *J. Neurosci.* 7:3474–3488.
43. Leterrier, J.-F., R. K. H. Liem, and M. L. Shelanski. 1981. Preferential phosphorylation of the 150,000 molecular weight component of neurofilaments by a cyclic AMP-dependent microtubule-associated protein kinase. *J. Cell Biol.* 90:755–760.
44. Deleted in proof.
45. Deleted in proof.
46. Lewis, S. A., M. G.-S. Lee, and N. J. Cowan. 1985. Five mouse tubulin isotypes and their regulated expression during development. *J. Cell Biol.* 101:852–861.
47. Lu, P.-W., C.-J. Soong, and M. Tao. 1985. Phosphorylation of ankyrin decreases its affinity for spectrin tetramer. *J. Biol. Chem.* 260:14958–14964.
48. Malik, M. N., M. D. Fenko, L. Scotto, P. Merz, J. Rothman, H. Tuzio, and H. M. Wisniewski. 1983. Purification and characterization of myosin from calf brain. *J. Neurochem.* 40:1620–1629.
49. Marotta, C. A., J. L. Harris, and J. M. Gilbert. 1978. Characterization of multiple forms of brain tubulin subunits. *J. Neurochem.* 30:1431–1440.
50. Marotta, C. A., P. Strocchi, and J. M. Gilbert. 1978. Microheterogeneity of brain cytoplasmic and synaptoplasmic actins. *J. Neurochem.* 30:1441–1451.
51. Matus, A., and B. Riderer. 1986. Microtubule-associated proteins in the developing brain. *Ann. NY Acad. Sci.* 466:167–169.
52. Morris, J. R., and R. J. Lasek. 1982. Stable polymers of the axonal cytoskeleton: the axoplasmic ghost. *J. Cell Biol.* 92:192–198.
53. Murthy, A. S. N., and M. Flavin. 1983. Microtubule assembly using the microtubule-associated protein MAP-2 prepared in defined states of phosphorylation with protein kinase and phosphatase. *Eur. J. Biochem.* 137:37–46.
54. Nelson, W. J., and E. Lazarides. 1984. The patterns of expression of two ankyrin isoforms demonstrate distinct steps in the assembly of the membrane skeleton in neuronal morphogenesis. *Cell.* 39:309–320.
55. Nestler, E. J., and P. Greengard. 1984. Protein phosphorylation in the nervous system. John Wiley & Sons Inc., New York.
56. Nixon, R. A. 1980. Protein degradation in the mouse visual system. I. Degradation of axonally transported and retinal proteins. *Brain Res.* 200:69–83.
57. Nixon, R. A. 1982. Increased axonal proteolysis in myelin-deficient mice. *Science (Wash. DC).* 215:999–1001.
58. Nixon, R. A. 1983. Proteolysis of neurofilaments. *In* Neurofilaments. C. A. Marotta, editor. University of Minnesota Press, Minneapolis. 117–154.
59. Nixon, R. A. 1987. The axonal transport of cytoskeletal proteins: a reappraisal. *In* Axonal Transport. M. A. Bisby and R. S. Smith, editors. Alan R. Liss Inc., New York. 175–200.
60. Nixon, R. A., and S. E. Lewis. 1986. Differential turnover of phosphate groups on neurofilament subunits in mammalian neurons *in vivo*. *J. Biol. Chem.* 261:16298–16301.
61. Nixon, R. A., and S. E. Lewis. 1987. Phosphorylation and dephosphorylation of neurofilament proteins in retinal ganglion cell neurons *in vivo*. *In* Molecular Mechanisms of Neuronal Responsiveness. Y. H. Ehrlich,

R. H. Lenox, E. Kornecki, and W. O. Berry, editors. Plenum Publishing Corp., New York. 167–186.
62. Nixon, R. A., and K. B. Logvinenko. 1986. Multiple fates of newly synthesized neurofilament proteins: evidence for a stationary neurofilament network distributed nonuniformly along axons of retinal ganglion cell neurons. *J. Cell Biol.* 102:647–659.
63. Nixon, R. A., B. A. Brown, and C. A. Marotta. 1982. Posttranslational modification of a neurofilament protein during axoplasmic transport: implications for regional specialization of CNS axons. *J. Cell Biol.* 94:150–158.
64. Nixon, R. A., B. A. Brown, and C. A. Marotta. 1983. Limited proteolytic modification of a neurofilament protein involves a proteinase activated by endogenous levels of calcium. *Brain Res.* 275:384–388.
65. Nixon, R. A., S. E. Lewis, D. Dahl, C. A. Marotta, and U. C. Drager. 1989. Early posttranslational modifications of the three neurofilament subunits in mouse retinal ganglion cells: neuronal sites and time course in relation to subunit polymerization and axonal transport. *Mol. Brain Res.* In press.
66. Nixon, R. A., S. E. Lewis, and C. A. Marotta. 1987. Posttranslational modification of neurofilament proteins by phosphate during axoplasmic transport in retinal ganglion cell neurons. *J. Neurosci.* 7:1145–1158.
67. Nixon, R. A., R. Quackenbush, and A. Vitto. 1986. Multiple calcium-activated neutral proteinases (CANP) in mouse retinal ganglion cell neurons: specificities for endogenous neuronal substrates and comparison to purified brain CANP. *J. Neurosci.* 6:1252–1263.
68. Nunez, J. 1986. Differential expression of microtubule components during brain development. *Dev. Neurosci.* 8:125–141.
69. Oblinger, M. M. 1987. Characterization of posttranslational processing of the mammalian high-molecular-weight neurofilament protein *in vivo*. *J. Neurosci.* 7:2510–2521.
70. Olmsted, J. B. 1986. Microtubule-associated proteins. *Annu. Rev. Cell Biol.* 2:421–457.
71. Pachter, J. S., and R. K. H. Liem. 1984. The differential appearance of neurofilament triplet polypeptides in the developing rat optic nerve. *Dev. Biol.* 103:200–210.
72. Pruss, R. M., R. Mirsky, M. C. Raff, R. Thorpe, A. J. Dowding, and B. H. Anderton. 1981. All classes of intermediate filaments share a common antigenic determinant defined by a monoclonal antibody. *Cell* 27: 419–428.
73. Raybin, D., and M. Flavin. 1977. Modification of tubulin by tyrosylation in cells and extracts and its effect on assembly in vitro. *J. Cell Biol.* 73:492–504.
74. Seldon, S. C., and T. D. Pollard. 1983. Phosphorylation of microtubule-associated proteins regulates their interaction with actin filaments. *J. Biol. Chem.* 258:7064–7071.
75. Sharp, G. A., G. Shaw, and K. Weber. 1982. Immunoelectron microscopical localization of the three neurofilament triplet proteins along neurofilaments of cultured dorsal root ganglion neurones. *Exp. Cell Res.* 137:403–413.
76. Shea, T. B., R. K. Sihag, and R. A. Nixon. 1988. Neurofilament triplet proteins of NB2/d1 neuroblastoma: posttranslational modification and incorporation into the cytoskeleton during differentiation. *Dev. Brain Res.* 43:97–109.
77. Shecket, G., and R. J. Lasek. 1982. Neurofilament protein phosphorylation. Species generality and reaction characteristics. *J. Biol. Chem.* 257:4788–4795.
78. Shelanski, M. L., and R. K. H. Liem. 1979. Neurofilaments. *J. Neurochem.* 33:5–13.
79. Sihag, R. K., and R. A. Nixon. 1989. *In vivo* phosphorylation of distinct domains of the 70 kilodalton neurofilament subunit involves different protein kinases. *J. Biol. Chem.* In press.
80. Sternberger, L. A., and N. H. Sternberger. 1983. Monoclonal antibodies distinguish phosphorylated and nonphosphorylated forms of neurofilaments *in situ*. *Proc. Natl. Acad. Sci. USA.* 80:6126–6130.
81. Strocchi, P., D. Dahl, and J. M. Gilbert. 1982. Studies on the biosynthesis of intermediate filament proteins in the rat CNS. *J. Neurochem.* 39:1132–1141.
82. Toyoshima, I., M. Satale, and T. Miyatake. 1984. Differences in the neurofilament proteins between perikaryon and axon of the bovine spinal ganglion. *Biomed. Res.* 5:459–464.
83. Traub, P., editor. 1985. Intermediate Filaments. A Review. Springer-Verlag New York Inc. 266 pp.
84. Trojanowski, J. Q., N. Walkenstein, and V. M.-Y. Lee. 1986. Expression of neurofilament subunits in the central and peripheral nervous system: an immunohistochemical study with monoclonal antibodies. *J. Neurosci.* 6:650–660.
85. Weber, K., G. Shaw, M. Osborn, E. Debus, and W. Geisler. 1983. Neurofilaments, a subclass of intermediate filaments: structure and expression. *Cold Spring Harbor Symp. Quant. Biol.* 48:717–729.
86. Willard, M. B. 1976. Genetically determined protein polymorphism in the rabbit nervous system. *Proc. Natl. Acad. Sci. USA.* 73:3641–3645.
87. Willard, M. B. 1983. Neurofilaments and axonal transport. *In* Neurofilaments. C. A. Marotta, editor. University of Minnesota Press, Minneapolis. 86–116.
88. Willard, M. B., and C. Simon. 1981. Antibody decoration of neurofilaments. *J. Cell Biol.* 89:198–205.
89. Willard, M. B., and C. Simon. 1983. Modulations of neurofilament axonal transport during the development of rabbit retinal ganglion cells. *Cell.* 36:551–559.
90. Zagon, I. S., R. Higbee, B. M. Riederer, and S. R. Goodman. 1986. Spectrin subtypes in mammalian brain: an immunoelectron microscopic study. *J. Neurosci.* 6:2977–2986.